Article ID: 1003－6326(2005)03－0671－09

Structure and bonding orientation of favorable growth unit $Al_6(OH)_{18}(H_2O)_6$ of gibbsite①

WU Zheng-ping(吴争平), CHEN Qi-yuan(陈启元),
YIN Zhou-lan(尹周澜), LI Jie(李 洁)
(School of Chemistry and Chemical Engineering, Central South University,
Changsha 410083, China)

Abstract: Three possible structures of the favorable growth unit $Al_6(OH)_{18}(H_2O)_6$ of gibbsite are calculated by *ab initio* at STO-3G, STO-3G*, STO-6G, STO-6G*, 3-21G, 6-31G levels and DFT at RB3LYP/3-21G, B3LYP/6-31G levels. The most excellent structure of $Al_6(OH)_{18}(H_2O)_6$(structure [A]) is confirmed. Based on these calculation results and considering efficiency factor, *ab initio* at STO-3G level is selected to optimize the structure [A]. The calculation results are compared with the experimental structure parameters of correlative systems. The total energy, orbital population and atomic charge of structure [A] are calculated using Dipole & Sphere solvent model at 6-31G, B3LYP/6-31G, 6-31G*, B3LYP/6-31G*, 6-31G** and B3LYP/6-31G** levels. The bonding orientation of $Al_6(OH)_{18}(H_2O)_6$ is analyzed.

Key words: gibbsite; *ab initio*; density fuction theory(DFT); structure; orientation
CLC number: O 641.12 **Document code:** A

1 INTRODUCTION

The crystal growth characteristics of gibbsite in supersaturated sodium aluminate solution were extensively investigated[1-5], but the structure and form of the growth unit were not related. Firstly, Vanstraten et al[6] indicated that the growth unit transition state of aluminate acid radical existed in the crystallization of gibbsite from alkaline sodium aluminate solution. Parkinson et al[7] figured out that $Al(OH)_4^-$, $Al(OH)_5^{2-}$ and $Al(OH)_6^{3-}$ would be likely to become growth units of gibbsite from the view point of crystal surface binding energy and it was the key problem to detect the decomposition mechanism of supersaturated sodium aluminate solution. A series of research results about growth units of gibbsite were reported[8-14] and at the same time they brought forward and proved that the growth units of gibbsite were $Al(OH)_6^{3-}$ and $Al(OH)_6^{3-}$ polymer, and $Al_6(OH)_{18}(H_2O)_6$ with hexagon face shape was the favorable growth unit. In this paper, based on investigation results by LI et al, the structure and bonding orientation of the favorable growth unit $Al_6(OH)_{18}(H_2O)_6$ of gibbsite are studied using *ab intio* and DFT methods by Gaussian98 on C2 workstation. This study may establish the foundation for discussing on the chemical bond force characteristics of gibbsite combination process.

2 CALCULATION METHODS

Based on *ab initio* Self Consistent Field molecular orbital theory, the total energy, dipole moment, orbital population and atomic charge are calculated at 6-31G, B3LYP/6-31G, 6-31G*, B3LYP/6-31G*, 6-31G**, B3LYP/6-31G** levels with Dipole & Sphere solvent model. Density Function Theory method adopts B3LYP Becke model with three parameters[15, 16]: an exchange functional[17] that consists of 20% Hartree-Fock Exchange, 8% Slater Exchange and 72% Becke-88 Exchange; and a correlation functional[18] that consists of 19% VWN# 5 Correlation and 81% LYP Correlation. This unusual combination is empirically determined by comparing with the results of very accurate calculations. All calculations are performed at C2 workstation in Central South University by Gaussian98 program.

The geometry optimization is implemented in several different levels:

1) Based on the Molecular Mechanics Force Field, the geometry optimization is implemented rudely by MM+ method. The MM+ force field is an extension of MM2 developed by Allinger and coworkers[19, 20] and is designed primarily for small organic molecules although it is expanded to peptides[21] and other systems as well[22]. In this paper, MM+ force field uses the latest MM2 (1991)

① **Foundation item:** Project(50374078) supported by the National Natural Science Foundation of China; Project(G1999064902) supported by the National Basic Research Program of China
Received date: 2004－04－31; **Accepted date:** 2004－12－30
Correspondence: WU Zheng-ping, PhD; Tel: +86-731-8877364-315; E-mail: wzp@mail.csu.edu.cn

parameters and atom types with the functional form[23-25] modified to incorporate nonbonded cutoffs(using switched or shifted smoothing), periodic boundary conditions, and the bond stretch term switched from cubic form to quadratic form in long range(to avoid the long range repulsive region of standard MM2).

2) Using *ab initio* Self Consistent Field method, the geometry optimization is implemented with STO-3G basis set.

3 STRUCTURE AND GEOMETRY OPTIMIZATION OF $Al_6(OH)_{18}(H_2O)_6$

3.1 Structure of $Al_6(OH)_{18}(H_2O)_6$

Based on the Molecular Mechanics Force Field, the geometry optimization is implemented rudely by MM+ method. Fig. 1 shows three possible optimized models of $Al_6(OH)_{18}(H_2O)_6$. The structures [A], [B] and [C] have H_2O—Al bond, H—O—H ··· H—O—Al hydrogen bond, and H_2O—H—O—Al bond respectively. Three possible structures are calculated by *ab initio* at STO-3G, STO-3G*, STO-6G, STO-6G*, 3-21G, 6-31G levels and DFT at RB3LYP/3-21G, B3LYP/6-31G levels. The calculation results of total energy and dipole moment are listed in Table 1.

The effect of the basis set selection on calculation of total energy by *ab initio* is obvious and the results of total energy would be improved when using diffuse functions. The numerical relation of

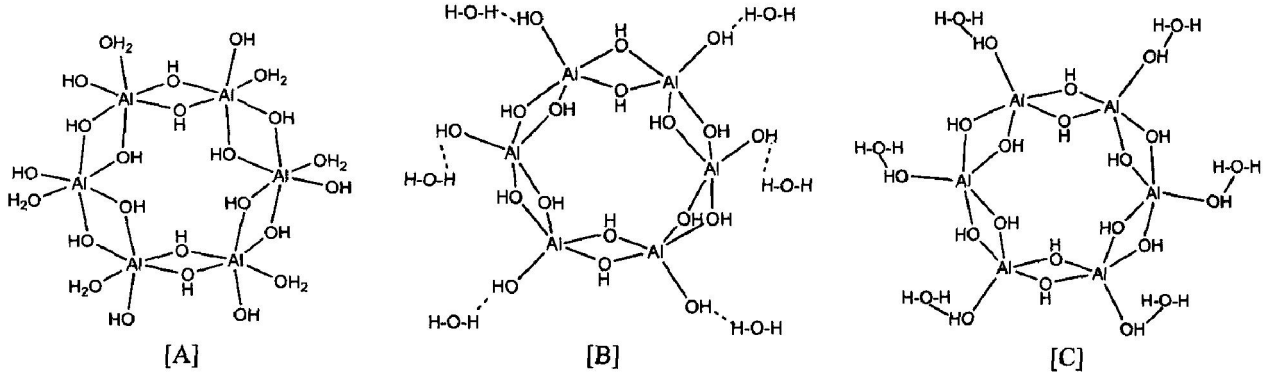

Fig. 1 Optimized structure models of $Al_6(OH)_{18}(H_2O)_6$ by MM+ method based on Molecular Mechanics Force Field

Table 1 Total energy and dipole moment of three possible structures of $Al_6(OH)_{18}(H_2O)_6$

Level	$Al_6(OH)_{18}(H_2O)_6$-[A]		$Al_6(OH)_{18}(H_2O)_6$-[B]		$Al_6(OH)_{18}(H_2O)_6$-[C]	
	Total energy/ ($kJ \cdot mol^{-1}$)	Total dipole moment/ Debye	Total energy/ ($kJ \cdot mol^{-1}$)	Total dipole moment/ Debye	Total energy/ ($kJ \cdot mol^{-1}$)	Total dipole moment/ Debye
RHF/STO-3G	−8 472 938.29	13.24	−8 469 896.95	4.06	−8 469 076.30	8.34
RHF/STO-3G*	−8 475 988.52	13.07	−8 472 619.03	4.21	−8 473 208.87	9.40
RHF/STO-6G	−8 548 910.88	13.35	−8 545 863.79	4.14	−8 546 351.57	9.44
RHF/STO-6G*	−8 551 988.32	13.18	−8 548 433.56	4.29	−8 549 218.62	9.43
RHF/3-21G	−8 537 194.73	14.02	−8 534 375.16	5.40	−8 534 917.74	11.94
RHF/3-21G/ SCRF= Dipole	−8 537 225.92	15.22	−8 534 379.89	5.96	−8 534 984.63	12.88
RB3LYP/3-21G	−8 568 962.81	12.41	−8 566 582.42	4.15	−8 567 087.98	11.26
RB3LYP/3-21G/ SCRF= Dipole	−8 568 990.06	13.97	−8 566 585.26	4.75	−8 567 105.91	12.66
RHF/6-31G	−8 580 921.82	14.19	−8 578 318.14	5.51	−8 578 917.97	12.00
RHF/6-31G/ SCRF= Dipole	−8 580 954.01	15.52	−8 578 323.53	6.20	−8 578 945.96	13.56
RB3LYP/6-31G	−8 613 640.21	12.69	−8 611 515.53	4.38	−8 611 992.63	11.28
RB3LYP/6-31G/ SCRF= Dipole	−8 613 666.35	14.26	−8 611 519.08	5.14	−8 612 011.97	12.85

total energy is $E_{(6\text{-}31G)} < E_{(STO\text{-}6G^*)} < E_{(STO\text{-}6G)} < E_{(3\text{-}21G)} < E_{(STO\text{-}3G^*)} < E_{(STO\text{-}3G)}$. With the same basis set, the DFT method adopting B3LYP model is better than *ab initio*. The numerical relation of total energy is $E_{(B3LYP/3\text{-}21G)} < E_{(3\text{-}21G)}$, $E_{(B3LYP/6\text{-}31G)} < E_{(6\text{-}31G)}$. Considering solvent effect and using Dipole & Sphere solvent model, the calculating results of total energy are all better than those on the condition of vacuum with the same basis set by DFT and *ab initio* methods. The numerical relation of total energy is $E_{(B3LYP/3\text{-}21G/SCRF=\ Dipole)} < E_{(B3LYP/3\text{-}21G)}$, $E_{(3\text{-}21G/SCRF=\ Dipole)} < E_{(3\text{-}21G)}$, $E_{(B3LYP/6\text{-}31G/SCRF=\ Dipole)} < E_{(B3LYP/6\text{-}31G)}$, $E_{(6\text{-}31G/SCRF=\ Dipole)} < E_{(6\text{-}31G)}$.

The numerical relation of dipole moments(p) of three possible structures of $Al_6(OH)_{18}(H_2O)_6$ is $p_{[A]} > p_{[C]} > p_{[B]}$ and the trend of change is consistent(see Table 1). Not only the chemical bonding but also the various Van der Waals forces exist on the precipitation of gibbsite in supersaturated sodium aluminate solution. $Al_6(OH)_{18}(H_2O)_6$ belongs to C1 group which is a typical polarity molecular without axis and side of symmetry. The orientation, inducement, and dispersion energy are directly proportional to quartic of dipole moment, square of polarization rate and dipole moment, square of polarization rate respectively. The polarization rate is directly proportional to cube of average molecular radius[26]. Fig. 2 shows the calculation results of average molecular radius. The calculation result of radius is 0.5 Å larger than the actual computed value. The radii of three possible structures of $Al_6(OH)_{18}(H_2O)_6$ are nearly between 5.06 Å and 5.83 Å as a result of the minimal difference of polarization rate. In a word, if the dipole moment becomes higher and higher, the Van der Waals forces would be larger and larger, and this would be advantageous to combination of the growth units of gibbsite. In addition, Fig. 3 shows the calculation results of electronic spatial extent (S). It can be seen from Fig. 3 that the numerical relation is $S_{[A]} < S_{[C]} < S_{[B]}$, which means that the framework of structure [A] is more compact than the others.

In sum of the calculation results and considering reliability of calculation method, the better structure is $Al_6(OH)_{18}(H_2O)_6$-[A].

3.2 Geometry optimization of structure [A]

Based on these calculation results and considering efficiency factor, *ab initio* method at STO-3G level is selected to optimize the structure [A]. The calculation results are compared with experiment structure parameters of correlation systems.

Experiment results of Al—O band length of sodium aluminate solution with various concentrations by solution X-ray diffractometry[14] are listed in Table 2. The band length of Al—O band in

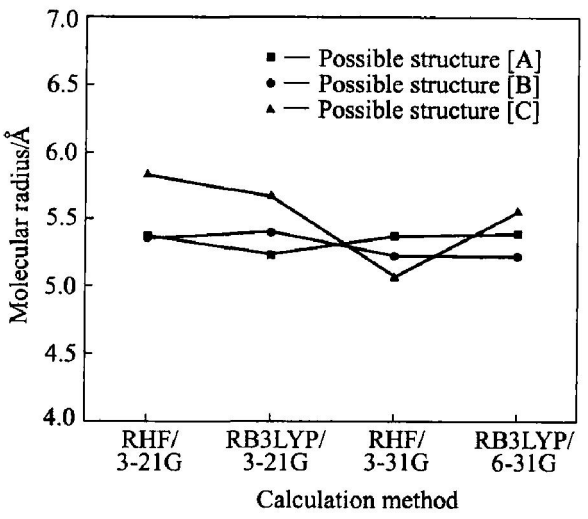

Fig. 2 Molecular radius of three possible structures of $Al_6(OH)_{18}(H_2O)_6$

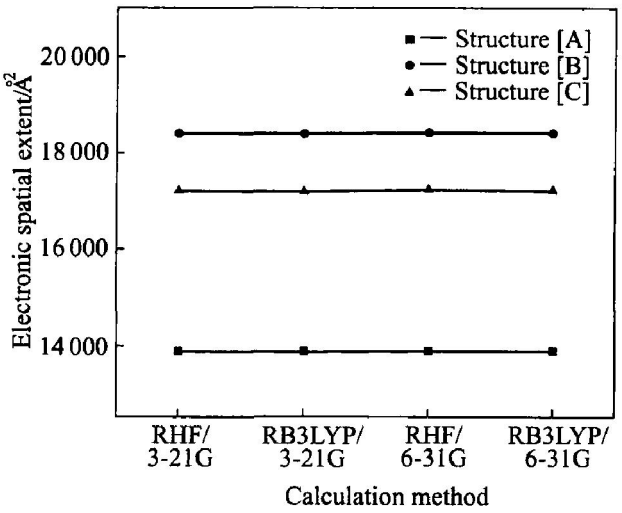

Fig. 3 Electronic spatial extent of three possible structures of $Al_6(OH)_{18}(H_2O)_6$

crystal $K_2[Al_2O(OH)_6]$, $Na_2[Al(OH)_4]Cl$ and $Na_{17}Al_5O_{16}$ are 1.73 - 1.78 Å, 1.756 Å and 1.80 Å respectively[27]. Al—O band length of structure [A] calculated by *ab initio* at RHF/STO-3G level and MM+ method based on the Molecular Mechanics Force Field are also listed in Table 3. It can be seen obviously from Table 3 that the band length of Al—O band calculated by *ab initio* at RHF/STO-3G level is more approachable with the experiment structure parameter than by MM+. That is to say that the results calculated at higher basis set would be rational. Fig. 4 shows the calculation model of the structure [A] optimized by *ab initio* at RHF/STO-3G level.

4 CALCULATION RESULTS AND DISCUSSION

4.1 Total energy

Fig. 5 shows the total energy of the structure [A] calculated at 6-31G, B3LYP/6-31G, $6\text{-}31G^*$, B3LYP/$6\text{-}31G^*$, $6\text{-}31G^{**}$, B3LYP/$6\text{-}31G^{**}$ levels

Table 2 Experiment results of Al—O band length of sodium aluminate solution with various concentrations by solution X-ray diffractometry[14]

Parameter	A(4.1)	B(4.2)	C(3.9)	D(3.6)	E(3.5)
c_{NaOH}/(mol·L^{-1})	2.426	3.639	4.852	5.822	7.278
$c_{Al(OH)_3}$/(mol·L^{-1})	1.700	2.550	3.400	4.080	4.100
Band length/Å	1.81	1.84	1.88	1.80	1.75

It is coordination number(n_{Al-O}) in bracket

Table 3 Calculation results of Al—O band length of structure [A]

Band	Bond length/Å		Band	Bond length/Å		Band	Bond length/Å	
	MM+ method	STO-3G method		MM+ method	STO-3G method		MM+ method	STO-3G method
Al_{11}—O_{29}	1.853 76	1.723 49	Al_{15}—O_{18}	1.852 66	1.774 74	Al_8—O_{27}	1.854 39	1.746 80
Al_{15}—O_{28}	1.852 47	1.798 99	Al_{15}—O_{16}	1.853 70	1.796 20	Al_8—O_{22}	1.853 00	1.774 50
Al_{23}—O_{27}	1.851 63	1.720 42	Al_{23}—O_{20}	1.852 70	1.824 83	Al_8—O_{18}	1.854 63	1.788 60
Al_{20}—O_{26}	1.851 77	1.715 78	Al_{23}—O_{18}	1.853 87	1.912 06	Al_8—O_9	1.854 10	1.814 49
Al_8—O_{25}	1.851 23	1.780 87	Al_{23}—O_{27}	1.853 28	1.822 61	Al_7—O_9	1.853 63	1.815 14
Al_7—O_{30}	1.852 52	1.788 38	Al_{23}—O_{19}	1.853 15	1.816 90	Al_7—O_{18}	1.852 50	1.790 66
Al_{11}—O_{17}	1.852 86	1.837 03	Al_{20}—O_{19}	1.853 66	1.827 10	Al_7—O_{12}	1.853 10	1.777 80
Al_{11}—O_{14}	1.856 14	1.816 49	Al_{20}—O_{20}	1.853 91	1.830 22	Al_7—O_{13}	1.852 10	1.769 30
Al_{15}—O_{17}	1.852 60	1.797 60	Al_{20}—O_{21}	1.853 90	1.855 97	Al_{11}—O_{12}	1.854 04	1.847 67
Al_{15}—O_{14}	1.854 83	1.780 90	Al_{20}—O_{22}	1.851 60	1.853 66	Al_{11}—O_{11}	1.853 10	1.838 18

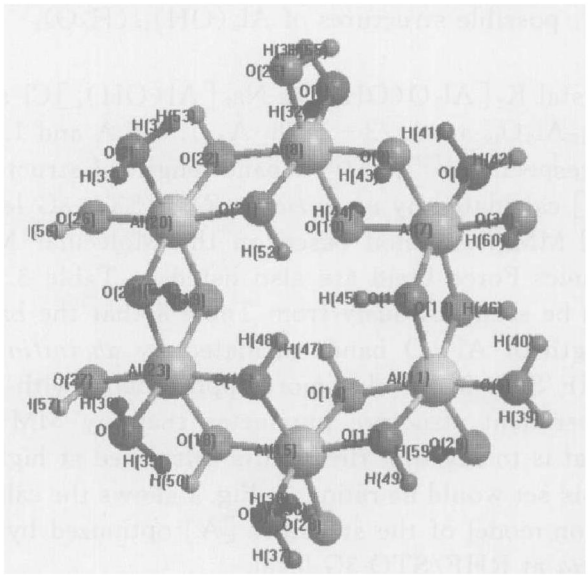

Fig. 4 Calculation model of $Al_6(OH)_{18}(H_2O)_6$-[A]

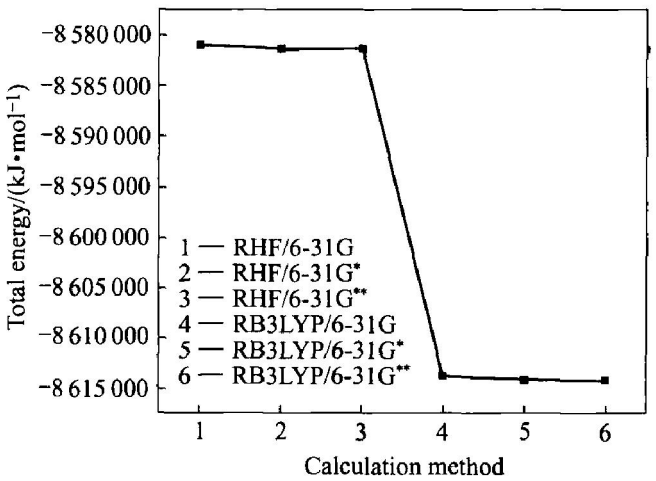

Fig. 5 Calculated total energy of structure [A] by *ab initio* and DFT

using Dipole & Sphere solvent model. When calculating total energy, DFT is better than *ab intio*. When the same basis sets is adopted, it would be improved slightly using diffusing functions. In other words, on the view point of energy for $Al_6(OH)_{18}(H_2O)_6$, DFT at B3LYP/6-31G level may be a better choice.

4.2 Atomic charge

The calculated results of atomic charge are listed in Table 4. When using diffusing functions, the effects on the atomic charge are so observable, and these effects are larger for Al, oxygen atoms in terminal and bridge OH groups than hydrogen and oxygen atoms in six H_2O. Adopting B3LYP three parameters model, the absolute value of negative charge and positive charge become smaller than using *ab initio* at same basis set level. In $Al_6(OH)_{18}(H_2O)_6$ (see Fig. 4), the hydrogen atoms of No. 31 to No. 41, No. 43 to No. 54, No. 55 to No. 60 are located at six H_2O, bridge OH groups, terminal OH groups respectively. It can be seen from Table 4 that the average value of atomic charge of the bridge hydrogen is larger than that of terminal hydrogen. Therefore from the viewpoint of bonding possibility among molecules, bridge hydrogen would be advantageous to bonding than terminal hydrogen, and in other word, the favorable bonding orientation is located at the obverse side(see Fig. 6).

At the same time it can be seen that atomic charge of hydrogen in H_2O is larger and more homologous than that of the other two kinds of hydrogen. This shows that existence of six H_2O is favorable to the system's stability and this result is consistent with what considered by LI[14] that existence of the terminal bonding H_2O is precondition of steady presence of growth units in sodium aluminate solution.

4.3 Analysis of orbital population

2 s orbital populations, the highest occupation s orbits of oxygen in terminal and bridge OH groups, are listed in Table 5. No. 9 to No. 24 and No. 25 to No. 30 are oxygen atoms in bridge and terminal OH groups respectively. 2 s orbital population of terminal oxygen is larger than bridge oxygen(see Table 5). 1s orbital populations, the highest occupation s orbits of hydrogen in terminal and

Table 4 Calculation results of atomic charge

No.	Atom	Calculation method					
		RHF /6-31G	RHF /6-31G*	RHF /6-31G**	RB3LYP /6-31G	RB3LYP /6-31G*	RB3LYP /6-31G**
1	O	- 0.894 527	- 0.748 615	- 0.707 816	- 0.722 010	- 0.541 732	- 0.465 056
2	O	- 0.860 629	- 0.700 383	- 0.712 091	- 0.691 925	- 0.460 973	- 0.437 389
3	O	- 0.861 015	- 0.755 843	- 0.717 600	- 0.695 376	- 0.523 892	- 0.450 715
4	O	- 0.894 018	- 0.676 285	- 0.657 890	- 0.718 192	- 0.445 902	- 0.405 783
5	O	- 0.864 650	- 0.645 741	- 0.611 928	- 0.701 523	- 0.393 730	- 0.336 774
6	O	- 0.892 987	- 0.752 992	- 0.731 188	- 0.728 494	- 0.514 430	- 0.478 399
7	Al	1.658 486	0.243 705	0.208 110	1.076 885	- 0.947 048	- 0.959 741
8	Al	1.629 403	- 0.040 715	- 0.126 749	1.016 925	- 1.209 624	- 1.306 045
9	O	- 1.095 848	- 0.677 793	- 0.633 352	- 0.865 779	- 0.257 088	- 0.150 693
10	O	- 1.103 234	- 0.852 876	- 0.777 401	- 0.878 542	- 0.424 739	- 0.326 165
11	Al	1.691 236	- 0.231 880	- 0.317 166	1.115 828	- 1.426 638	- 1.625 909
12	O	- 1.078 647	- 0.770 588	- 0.668 435	- 0.863 190	- 0.318 259	- 0.184 845
13	O	- 1.049 100	- 0.479 941	- 0.472 343	- 0.822 617	- 0.087 820	- 0.011 122
14	O	- 1.084 605	- 0.853 620	- 0.747 156	- 0.860 202	- 0.455 782	- 0.314 235
15	Al	1.617 764	- 0.154 954	- 0.413 708	0.992 254	- 1.272 897	- 1.612 651
16	O	- 1.121 937	- 0.867 517	- 0.771 685	- 0.894 631	- 0.399 810	- 0.282 619
17	O	- 1.101 811	- 0.377 435	- 0.311 013	- 0.874 205	0.035 254	0.144 935
18	O	- 1.037 599	- 0.460 053	- 0.362 814	- 0.813 623	- 0.052 240	0.087 658
19	O	- 1.150 341	- 0.680 940	- 0.581 561	- 0.913 640	- 0.147 026	- 0.038 405
20	Al	1.741 537	0.072 648	- 0.027 449	1.160 603	- 1.221 692	- 1.373 685

Continue

No.	Atom	Calculation method					
		RHF /6-31G	RHF /6-31G*	RHF /6-31G**	RB3LYP /6-31G	RB3LYP /6-31G*	RB3LYP /6-31G**
21	O	-1.104 198	-0.793 708	-0.633 487	-0.881 560	-0.292 273	-0.097 586
22	O	-1.085 842	-0.470 826	-0.352 687	-0.861 902	-0.077 856	0.084 098
23	Al	1.610 329	-0.079 551	-0.313 995	0.985 482	-1.411 905	-1.697 154
24	O	-1.085 198	-0.671 174	-0.543 595	-0.861 637	-0.227 001	-0.021 676
25	O	-1.006 590	-0.744 912	-0.600 338	-0.800 241	-0.490 752	-0.321 742
26	O	-0.960 781	-0.569 029	-0.497 751	0.764 039	0.307 172	-0.213 605
27	O	-0.951 709	-0.624 342	-0.556 467	-0.755 129	-0.347 971	-0.257 444
28	O	-1.001 348	-0.672 083	-0.586 303	-0.794 675	-0.431 105	-0.309 263
29	O	-1.010 011	-0.719 630	-0.639 452	-0.802 785	-0.462 181	-0.353 004
30	O	-0.995 630	-0.708 571	-0.606 843	-0.792 929	-0.443 792	-0.291 469
31	H	0.537 720	0.641 338	0.566 784	0.480 461	0.598 733	0.512 492
32	H	0.508 835	0.590 848	0.599 268	0.460 673	0.553 414	0.552 689
33	H	0.494 601	0.580 462	0.569 822	0.450 226	0.545 829	0.522 487
34	H	0.538 940	0.622 789	0.542 316	0.488 085	0.577 932	0.481 545
35	H	0.519 296	0.609 259	0.581 020	0.468 383	0.565 193	0.526 365
36	H	0.501 479	0.586 951	0.587 209	0.453 643	0.550 562	0.544 742
37	H	0.546 990	0.632 268	0.618 332	0.496 775	0.589 006	0.578 547
38	H	0.515 383	0.580 864	0.551 839	0.466 156	0.540 358	0.504 241
39	H	0.531 985	0.610 349	0.556 644	0.481 435	0.566 277	0.508 562
40	H	0.493 503	0.571 543	0.562 838	0.435 519	0.520 882	0.497 093
41	H	0.513 325	0.599 592	0.547 834	0.463 420	0.560 228	0.510 572
42	H	0.541 559	0.611 968	0.580 150	0.491 798	0.568 733	0.542 135
Average		0.520 3	0.603 2	0.572 0	0.469 7	0.561 4	0.523 5
43	H	0.502 628	0.589 996	0.598 300	0.459 068	0.567 645	0.515 450
44	H	0.455 786	0.539 776	0.465 534	0.410 732	0.525 504	0.381 417
45	H	0.416 482	0.467 638	0.365 527	0.369 231	0.441 977	0.273 987
46	H	0.479 675	0.554 436	0.568 027	0.446 008	0.534 654	0.499 841
47	H	0.464 248	0.619 502	0.564 989	0.411 142	0.605 365	0.528 075
48	H	0.449 551	0.509 646	0.511 999	0.389 131	0.476 382	0.479 851
49	H	0.497 625	0.547 650	0.600 027	0.458 795	0.519 501	0.556 653
50	H	0.466 400	0.538 826	0.523 983	0.436 427	0.520 871	0.479 261
51	H	0.541 725	0.616 573	0.555 458	0.493 340	0.589 528	0.484 111
52	H	0.453 076	0.467 422	0.462 516	0.405 069	0.438 631	0.434 560
53	H	0.491 402	0.548 478	0.499 784	0.454 625	0.527 098	0.463 749
54	H	0.440 643	0.522 956	0.614 960	0.399 734	0.505 798	0.545 720
Average		0.471 6	0.570 9	0.527 6	0.427 8	0.521 1	0.470 2
55	H	0.426 889	0.469 902	0.366 809	0.390 382	0.449 208	0.342 348
56	H	0.381 678	0.413 433	0.307 263	0.355 276	0.394 986	0.276 944
57	H	0.373 959	0.410 673	0.354 629	0.347 332	0.392 393	0.342 166
58	H	0.413 506	0.458 070	0.403 538	0.377 831	0.433 386	0.362 942
59	H	0.429 754	0.484 376	0.432 484	0.389 152	0.453 028	0.384 761
60	H	0.414 857	0.468 060	0.412 269	0.381 020	0.444 977	0.373 177
Average		0.406 8	0.450 7	0.379 4	0.373 5	0.428 0	0.347 1

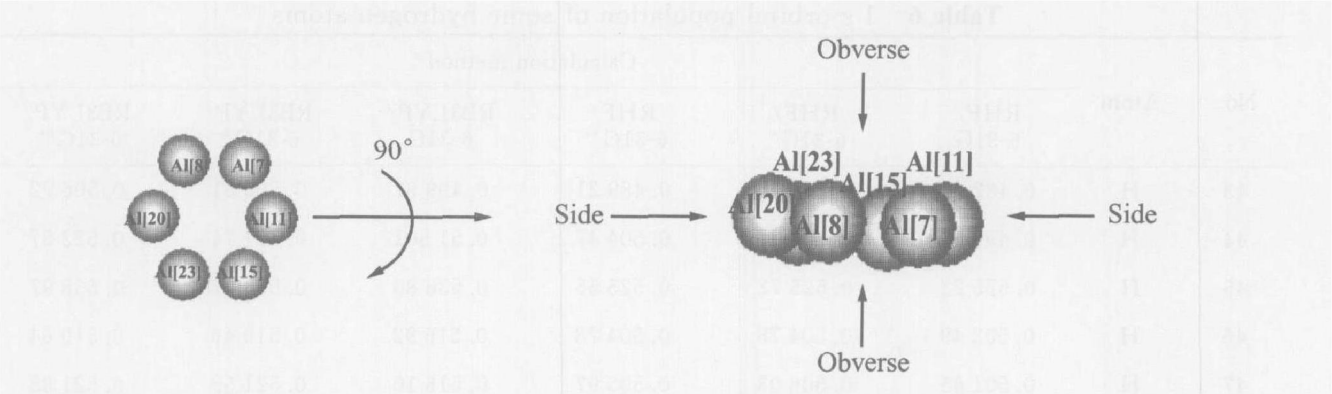

Fig. 6 Sketch map of bonding orientation

Table 5 2 s orbital population of some oxygen atoms

No.	Atom	Calculation method					
		RHF/ 6-31G	RHF/ 6-31G*	RHF/ 6-31G**	RB3LYP/ 6-31G	RB3LYP/ 6-31G*	RB3LYP/ 6-31G**
9	O	0.854 88	0.843 58	0.842 40	0.871 80	0.862 94	0.861 87
10	O	0.858 08	0.846 01	0.845 22	0.875 29	0.865 49	0.864 78
12	O	0.859 86	0.850 67	0.849 94	0.876 85	0.870 20	0.869 59
13	O	0.862 99	0.849 42	0.848 10	0.880 18	0.868 63	0.867 42
14	O	0.862 96	0.851 56	0.850 16	0.880 44	0.871 18	0.869 93
16	O	0.852 41	0.843 90	0.842 98	0.869 83	0.863 35	0.862 50
17	O	0.856 52	0.843 27	0.842 41	0.873 49	0.862 47	0.861 71
18	O	0.865 13	0.852 58	0.851 32	0.882 58	0.872 04	0.870 91
19	O	0.848 67	0.835 80	0.835 36	0.865 68	0.855 15	0.854 80
21	O	0.855 93	0.846 44	0.845 52	0.872 90	0.865 99	0.865 20
22	O	0.860 11	0.847 46	0.845 96	0.877 12	0.866 45	0.865 05
24	O	0.864 13	0.851 59	0.849 37	0.881 36	0.871 25	0.869 15
Average		0.858 47	0.846 86	0.845 65	0.875 63	0.866 26	0.865 24
25	O	0.869 79	0.861 39	0.860 48	0.887 96	0.881 28	0.880 43
26	O	0.877 19	0.867 87	0.867 62	0.894 80	0.887 62	0.887 42
27	O	0.878 39	0.868 87	0.868 64	0.895 94	0.888 61	0.888 44
28	O	0.867 21	0.858 88	0.858 28	0.884 43	0.878 50	0.878 00
29	O	0.866 79	0.858 11	0.857 45	0.883 86	0.877 70	0.877 13
30	O	0.871 38	0.861 79	0.861 14	0.889 04	0.881 74	0.881 21
Average		0.871 79	0.862 82	0.862 27	0.889 34	0.882 58	0.882 11

bridge OH groups, are listed in Table 6. 1 s orbital population of terminal hydrogen is larger than bridge hydrogen(see Table 6). The population analysis is hereby given that terminal OH group is steadier than bridge OH group. From the view point of inter-molecular bonding orientation, bridge OH group is easier to bond and the favorable bonding orientation is located at the obverse side(see Fig. 6). The conclusion is consistent with the analysis result in 4. 2.

Table 6 1 s orbital population of some hydrogen atoms

No.	Atom	Calculation method					
		RHF/6-31G	RHF/6-31G*	RHF/6-31G**	RB3LYP/6-31G	RB3LYP/6-31G*	RB3LYP/6-31G**
43	H	0.482 21	0.489 50	0.489 21	0.499 67	0.506 81	0.506 72
44	H	0.498 11	0.503 86	0.504 47	0.51 501	0.521 74	0.522 57
45	H	0.525 22	0.525 72	0.525 55	0.536 80	0.538 87	0.538 97
46	H	0.502 49	0.504 78	0.504 78	0.516 92	0.519 49	0.519 64
47	H	0.501 65	0.506 03	0.505 97	0.516 10	0.521 59	0.521 85
48	H	0.510 13	0.513 24	0.512 99	0.524 03	0.528 09	0.527 99
49	H	0.486 23	0.490 82	0.491 55	0.503 02	0.507 98	0.508 83
50	H	0.508 94	0.510 91	0.511 27	0.522 47	0.525 27	0.525 75
51	H	0.459 36	0.469 38	0.470 45	0.479 86	0.490 98	0.492 16
52	H	0.517 32	0.518 39	0.518 33	0.529 47	0.532 48	0.532 58
53	H	0.495 20	0.498 98	0.499 03	0.510 79	0.514 69	0.514 90
54	H	0.507 37	0.510 40	0.509 61	0.521 58	0.524 80	0.524 18
Average		0.499 52	0.503 50	0.503 60	0.514 64	0.519 40	0.519 68
55	H	0.508 05	0.509 86	0.509 33	0.521 76	0.523 45	0.523 07
56	H	0.526 84	0.525 24	0.524 53	0.537 63	0.536 61	0.536 07
57	H	0.530 30	0.529 30	0.528 79	0.540 37	0.540 15	0.539 90
58	H	0.503 61	0.507 13	0.507 31	0.517 39	0.521 48	0.521 76
59	H	0.499 77	0.504 29	0.504 59	0.514 29	0.519 55	0.520 06
60	H	0.508 50	0.512 26	0.511 85	0.521 32	0.525 27	0.525 15
Average		0.512 85	0.514 68	0.514 40	0.525 46	0.527 75	0.527 67

5 CONCLUSIONS

1) Geometry optimization on $Al_6(OH)_{18}(H_2O)_6$ is performed at RHF/STO-3G level and the calculation structure parameters are relatively approachable with the experimental values.

2) Total energy of $Al_6(OH)_{18}(H_2O)_6$ is calculated at 6-31G, B3LYP/6-31G, 6-31G*, B3LYP/6-31G*, 6-31G**, B3LYP/6-31G** levels using Dipole & Sphere solvent model. From the view point of energy, DFT method is better than *ab initio* and the effect of using diffuse functions on energy calculation is not obvious.

3) Atomic charge and orbital population are calculated using Dipole & Sphere solvent model. All calculation results indicate that bridge OH group is easier to bond, and the favorable bonding orientation is located at the bridge OH group orientation.

REFERENCES

[1] Fleming S, Rohl A. Atomistic modeling of gibbsite: surface structure and morphology [J]. J Light Metal, 1998(CD-ROM and Bound Volume Set): 167-173.

[2] Gerson A, Ralston J. Investigation of the mechanism of gibbsite nucleation using molecular modeling [J]. Colloids and Sueface A: Physico Chemical and Engineering Aspects, 1996, 110: 105-117.

[3] Misra C, White E T. Kinetics of crystallization of aluminum trihydraoxide from seeded caustic aluminate solution [J]. Chem Eng Progr Sympos Ser, 1970, 110: 53.

[4] Brown N. A quantitative study of new crystal formation in seeded caustic aluminate solutions [J]. Journal of Crystal Growth, 1975, 29: 309-405.

[5] Brown N. Crystal growth and nucleation of aluminum trihydraoxide from seeded caustic aluminate solutions [J]. Journal of Crystal Growth, 1972, 12: 39-45.

[6] Vanstraten H A, Schoonen M A A. Precipitation from supersaturated aluminate solutions(Ⅳ)—Influence of citrate ions [J]. J Colloid and Interface Science, 1985, 106(1): 175-185.

[7] Fleming S, Parkinson G. Atomistic modeling of gibbsite: surface structure and morphology [J]. Journal of Crystal Growth, 2000, 209: 159-166.

[8] LI Jie, CHEN Qi-yuan. Investigation on the mode of the growth unit for alumina trihydrate crystals precipitation from supersaturated sodium aluminate solution [A]. Hydrometallurgy, ICHM'98 [C]. China: Kunming, 240.

[9] LI Jie, CHEN Qi-yuan, YIN Zhou-lan. Studies on the

kinetics of unseeded nucleation of aluminum trihydroxide from supersaturated sodium aluminate solutions [J]. Chemical Journal of Chinese University, 2003, 24 (9): 1652 - 1656. (in Chinese).

[10] LI Jie, CHEN Qi-yuan, YIN Zhou-lan, et al. Development and prospect in the fundamental research on the decomposition of supersaturated sodium aluminate solution [J]. Progress in Chemistry, 2003, 15(3): 170 - 177. (in Chinese).

[11] CHEN Qi-yuan, LI Jie, YIN Zhou-lan, et al. Decomposition of supersaturated sodium aluminate solution [J]. Trans Nonferrous Metals Soc China, 2003, 13(3): 649 - 654.

[12] CHEN Qi-yuan, ZHOU Jun, LI Jie, et al. A theoretical investigation on the transformation of aluminate ions [J]. Trans Nonferrous Metals Soc China, 2003, 13(4): 812 - 818.

[13] CHEN Guo-hui, CHEN Qi-yuan, YIN Zhou-lan, et al. SEM observation of gibbsite precipitation with seeds from sodium aluminate solutions promoted by ultrasound [J]. Trans Nonferrous Met Soc China, 2003, 13(3): 708 - 714..

[14] LI Jie. Study on the Structure Characteristics and Decomposition Mechanism of Supersaturated Sodium Aluminate Solution [D]. Changsha: Central South University, 2001. 12. (in Chinese).

[15] Frisch M J, Trucks C W, Schlegel H W, et al. Gaussian Program [R]. Gaussian, Inc, Pittshurgh PA, 1998.

[16] Becke A D. Density-functional thermochemistry (Ⅲ) —the role of exact exchange [J]. J Chem Phys, 1993, 98(9): 5648 - 5702.

[17] Wada K, Masui R, Matsubara H, et al. Properties and structure of the soluble ferredoxin from Synechococcus 6301 (Anacystis nidulans), relationship to gene sequences [J]. J Biochem, 1988, 252 (2): 571 - 575.

[18] Becke A D. Density-functional exchange-energy approximation with correct asymptotic behavior [J]. Phys Rev A, 1988, 38(9): 3098 - 3100.

[19] Allinger N L, Yuh Y H, Lii J H. The MM3 force field for hydrocarbons [J]. J Am Chem Soc, 1989, 111(23): 8551 - 8566.

[20] Allinger N L. A Classic Introduction to Molecular Mechanics is Molecular Mechanics [A]. ACS Monograph177 [C]. American Chemical Society, 1982.

[21] Lii J H, Allinger N L. The MM3 force field for hydrocarbons: 2 vibrational frequencies and thermodynamics [J]. Journal of the American Chemical Society, 1989, 111(23): 8566 - 8575.

[22] Lipkowitz K B. Applications of Post-Hartree-Fock Methods: A tutorial [M]. QCPE Bulletin, Indiana University, 1992.

[23] Allinger N L. A hydrocarbon force field utilizing V1 and V2 torsional terms [J]. Journal of the American Chemical Society, 1977, 99(25): 8127 - 8134.

[24] Allinger N L, Rahman R, Lii J H. A molecular mechanics force field(MM3) for alcohols and ethers [J]. Journal of the American Chemical Society, 1990, 112 (23): 8293 - 8307.

[25] Besler B H, Merz M H Jr, Kollman P A. Atomic charges derived from semiempirical methods [J]. J Comp Chem, 1990, 11(2): 431 - 439.

[26] DENG Neng-wu, ZHANG Hong-lie, ZHAO Wei-rong. Physical Conception of Chemical Bond [M]. Anhui Technology Press, 1985. 199 - 208. (in Chinese).

[27] Moolenaar R J, Evans J G, Mckeever L D. The structure of the aluminate ion in solutions at high pH [J]. J Physical Chemistry, 1970, 74(6): 3629 - 3636.

(Edited by YANG Bing)